Human Molecular Genetics, 2018, Vol. 00, No. 00 1–12

doi: 10.1093/hmg/ddy293
Advance Access Publication Date: 12 September 2018
General Article

Downloaded from https://academic.oup.com/hmg/advance-article-abstract/doi/10.1093/hmg/ddy293/5068614 by Kyoto Daigaku Nogaku-bu Toshoshitsu user on 21 September 2018

GENERAL ARTICLE

A patient-derived iPSC model revealed oxidative stress increases facioscapulohumeral muscular dystrophy-causative *DUX4*

Mitsuru Sasaki-Honda[1,2], Tatsuya Jonouchi[1], Meni Arai[1,3], Akitsu Hotta[1], Satomi Mitsuhashi[4,5], Ichizo Nishino[5], Ryoichi Matsuda[2,6] and Hidetoshi Sakurai[1,*]

[1]Center for iPS Cell Research and Application (CiRA), Kyoto University, 53 Shogoin Kawahara-cho, Sakyo-ku, Kyoto 606-8507, Japan, [2]Department of Biological Sciences, Graduate School of Science, The University of Tokyo, 3-8-1 Komaba, Meguro, Tokyo 153-8902, Japan, [3]Agricultural and Environmental Engineering, Faculty of Agriculture, Kyoto University, Kitashirakawa Oiwake-cho, Sakyo-ku, Kyoto 606-8502, Japan, [4]Department of Human Genetics, Yokohama City University Graduate School of Medicine, Yokohama, Kanagawa 236-0004, Japan, [5]Department of Neuromuscular Research, National Institute of Neuroscience, National Center of Neurology and Psychiatry, Kodaira, Tokyo 187-8502, Japan and [6]Department of Life Sciences, Graduate School of Arts and Sciences, the University of Tokyo, 3-8-1 Komaba, Meguro, Tokyo 153-8902, Japan

*To whom correspondence should be addressed at: Center for iPS Cell Research and Application (CiRA), Kyoto University, 53 Shogoin Kawahara-cho, Sakyo-ku, Kyoto 606-8507, Japan. Tel: +81-75-366-7055; Fax: +81-75-366-7177; Email: hsakurai@cira.kyoto-u.ac.jp

Abstract

Double homeobox 4 (*DUX4*), the causative gene of facioscapulohumeral muscular dystrophy (FSHD), is ectopically expressed in the skeletal muscle cells of FSHD patients because of chromatin relaxation at 4q35. The diminished heterochromatic state at 4q35 is caused by either large genome contractions [FSHD type 1 (FSHD1)] or mutations in genes encoding chromatin regulators, such as *SMCHD1* [FSHD type 2 (FSHD2)]. However, the mechanism by which *DUX4* expression is regulated remains largely unknown. Here, using a myocyte model developed from patient-derived induced pluripotent stem cells, we determined that *DUX4* expression was increased by oxidative stress (OS), a common environmental stress in skeletal muscle, in both FSHD1 and FSHD2 myocytes. We generated FSHD2-derived isogenic control clones with SMCHD1 mutation corrected by clustered regularly interspaced short palindromic repeats (CRISPR)/ CRISPR associated 9 (Cas9) and homologous recombination and found in the myocytes obtained from these clones that *DUX4* basal expression and the OS-induced upregulation were markedly suppressed due to an increase in the heterochromatic state at 4q35. We further found that DNA damage response (DDR) was involved in OS-induced *DUX4* increase and identified ataxia-telangiectasia mutated, a DDR regulator, as a mediator of this effect. Our results suggest that the relaxed chromatin state in FSHD muscle cells permits aberrant access of OS-induced DDR signaling, thus increasing *DUX4* expression. These results suggest OS could represent an environmental risk factor that promotes FSHD progression.

Received: May 4, 2018. **Revised:** June 18, 2018. **Accepted:** August 7, 2018

©The Author(s) 2018. Published by Oxford University Press.
This is an Open Access article distributed under the terms of the Creative Commons Attribution Non-Commercial License (http://creativecommons.org/licenses/by-nc/4.0/), which permits non-commercial re-use, distribution, and reproduction in any medium, provided the original work is properly cited. For commercial re-use, please contact journals.permissions@oup.com

Introduction

Facioscapulohumeral muscular dystrophy (FSHD) is a genetically inherited disease that causes progressive weakness of the skeletal muscle. FSHD type 1 (FSHD1) is caused by reduced D4Z4 repeats (1–10 repeats) combined with permissive polymorphisms containing a polyadenylation (poly(A)) signal (PAS) at the sub-telomeric region 4q35. Similarly, FSHD type 2 (FSHD2) is caused by reduced D4Z4 repeats combined with permissive polymorphisms containing a PAS at 4q35, but the repeats exceed 10, and mutations in chromatin regulators, including *SMCHD1* (structural maintenance of chromosomes flexible hinge domain containing 1), are also present (1–3). The genomic mutations in both FSHD1 and FSHD2 result in chromatin relaxation at 4q35, which is characterized by DNA hypomethylation and a reduction in the levels of histone 3 lysine 9 trimethylation (H3K9me3) and heterochromatin protein 1γ (HP1γ). Thus, PAS stabilizes double homeobox 4 (*DUX4*) transcripts to permit ectopic expression of the gene (3–6). The aberrant *DUX4* expression exerts toxic effects in skeletal muscle cells through its transcriptional activity (7–9). FSHD1 and FSHD2 patients show similar clinical phenotypes, suggesting an identical molecular pathology (10).

FSHD shows unique clinical characteristics compared to other types of muscular dystrophies including relatively late onset of the disease phenotypes (typically during the second decade), asymmetric patterns of muscle weakness and large variations in disease progression among patients (11). This variability in symptoms is partially explained by the approximately inverse correlation between the number of D4Z4 repeats and clinical severity (12), but this explanation remains incomplete because clinical variability is found even among patients harboring the same number of D4Z4 repeats (13). Based on a series of clinical and genetic studies, the current consensus is that endogenous *DUX4* expression plays a causative role in FSHD pathogenesis; the varying clinical characteristics of the disease would strongly support the existence of exogenous factors that modulate the clinical phenotype by affecting events upstream or downstream of *DUX4* expression. Accordingly, a recent study showed that estrogens could function in mediating the sex-related differences in the disease by antagonizing DUX4 downstream events without altering *DUX4* expression, thus protecting against the impaired differentiation of patient-derived myoblasts (14). Regarding events upstream of *DUX4*, previous pharmacological studies have identified several upstream regulators of *DUX4* (15–18), but no extracellular factor that increases *DUX4* expression has been reported so far. Moreover, the low-level expression of DUX4 raises questions regarding its functional impact; only extremely few cultured cells (1/1000 cells) show detectable DUX4 expression at the translational level (19). Furthermore, to date, no evidence has been reported of DUX4 protein expression in FSHD patient biopsies. However, endogenous DUX4 expression was shown to be sufficient for inducing cellular toxicity during the differentiation of myoblasts into myotubes or for impairing the differentiation of pluripotent stem cells into cells of skeletal muscle lineage (20,21). Thus, low but substantial *DUX4* expression in cultured cells derived from distinct patients with FSHD appears to reflect differences in clonal conditions and disease progression of the patients (19). In addition, a recently reported rodent FSHD model showed that the muscular pathological phenotype depends on *DUX4* transgene expression levels (22). A consideration of these findings led us to hypothesize that an external factor modulates disease onset and progression in FSHD patients through the transcriptional regulation of *DUX4*.

Oxidative stress (OS) is one of the major stresses affecting skeletal muscle function in the context of both homeostasis and pathology (23,24). The involvement of OS in FSHD pathology is supported by certain clinical and experimental studies. Clinical studies have revealed that OS markers are elevated in FSHD muscle as compared with the level in healthy muscle (25) and that oral supplementation of antioxidants partially improves muscle function in FSHD patients (26). In addition, the results of *in vitro* experimental studies have shown that FSHD myoblasts are vulnerable to H_2O_2 stimulation, a model of OS, and that DUX4-induced endogenous OS contributes to aberrant differentiation (27–29). Moreover, a series of transcriptomic studies revealed that DUX4 altered the transcription of OS-response genes (30–32). Thus, the findings obtained to date have positioned OS downstream of DUX4 in FSHD pathology, but the possibility that OS affects *DUX4* expression by acting as an upstream factor has not been investigated.

In the present study, using myocytes differentiated from induced pluripotent stem cells (iPSCs) derived from both FSHD1 and FSHD2 patients, we demonstrated that OS increases *DUX4* expression specifically in FSHD muscle cells. By using genome-editing technology, we generated isogenic controls of FSHD2 iPSCs by correcting the *SMCHD1* mutation; myocytes derived from these isogenic controls showed suppressed basal DUX4 expression and partially recovered heterochromatic markers at 4q35. Notably, the OS-induced DUX4 increase was also suppressed in these gene-corrected myocytes. Lastly, we attributed the DUX4 increase by OS to aberrant access of DNA damage response (DDR) signaling to the opened FSHD 4q35 region and further identified ataxia-telangiectasia-mutated (ATM) kinase as a mediator of this effect. These results suggest that OS could represent an environmental risk factor that promotes FSHD progression through the regulation of *DUX4*.

Results

Generation of iPS$^{tet\text{-}MyoD}$ clones from FSHD1 and FSHD2 patients and a healthy control donor

We prepared iPSCs from one FSHD1 patient harboring three D4Z4 repeats (F1), one FSHD2 patient harboring an *SMCHD1* mutation (F2) and one healthy donor with no FSHD symptoms (HC) by using a previously established method, in which episomal vectors carrying the reprogramming factors Oct3/4, Sox2, Klf4 and L-Myc were transfected into skin fibroblasts of HC and F1 and blood cells of F2 (Supplementary Material, Table S1). To obtain iPSCs possessing the potential to efficiently differentiate into myocytes, we used a tetracycline-inducible MyoD piggyBac vector (tet-MyoD) that was constructed previously; this enabled the transfected iPSCs (iPS$^{tet\text{-}MyoD}$) to express MyoD, a master regulator gene for skeletal muscle differentiation, and subsequently to differentiate into myosin heavy chain (MyHC)-positive myocytes only when Dox was added to the medium (Fig. 1A) (33). The expression of stage-specific embryonic antigen (SSEA)-4 and tumor-related antigen (TRA)-1–60, which are indicators of undifferentiated pluripotent stem cells, was detected by immunocytochemistry, demonstrating that the iPS$^{tet\text{-}MyoD}$ clones retained undifferentiated pluripotent characteristics (Fig. 1B; Supplementary Material, Fig. S1A). To model myocytes, myogenic differentiation was performed on these iPS$^{tet\text{-}MyoD}$ clones through Dox-inducible MyoD overexpression. On day 8, >80% of the nuclei were positioned inside MyHC-positive cells in each clone, indicating that comparable myocyte lineage was induced from two iPS$^{tet\text{-}MyoD}$ clones from each donor (HC#1, HC#2, F1#1, F1#2, F2#1 and F2#2) (Fig. 1C and D; Supplementary Material, Fig. S1B

Downloaded from https://academic.oup.com/hmg/advance-article-abstract/doi/10.1093/hmg/ddy293/5068614 by Kyoto Daigaku Nogaku-bu Toshoshitsu user on 21 September 2018

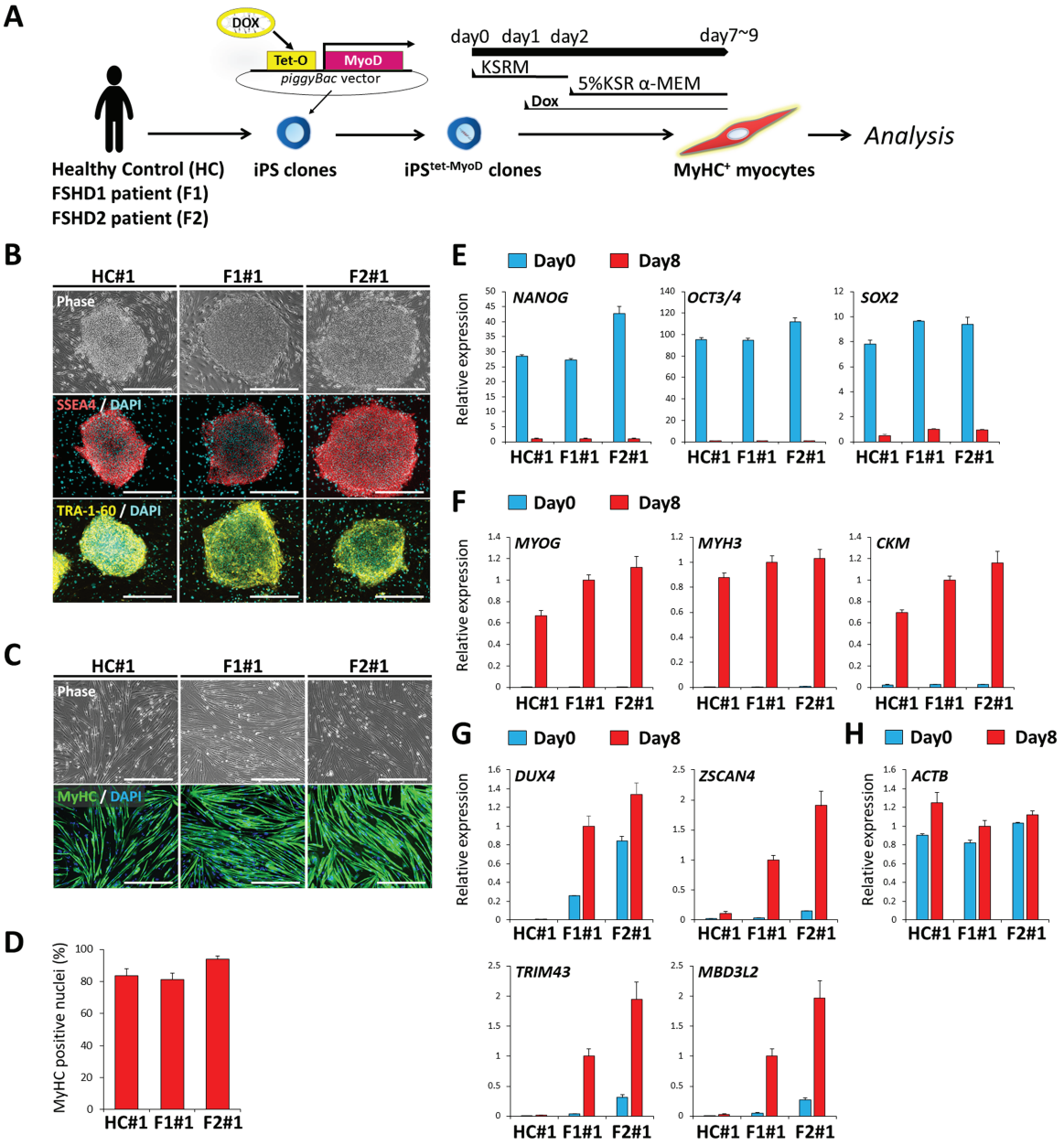

Figure 1. iPS$^{tet\text{-}MyoD}$ clones were generated from a healthy control and from FSHD1 and FSHD2 patients. (**A**) Scheme of the differentiation of iPSC clones to myocytes. (**B**) Representative images of immunofluorescence staining of SSEA4 (red) and TRA-1-60 (yellow) in undifferentiated iPSC$^{tet\text{-}MyoD}$ clones. Scale bar: 500 µm. (**C**) Representative images of immunofluorescence staining of MyHC (green) in differentiated myocytes at day 8. Scale bar: 500 µm. (**D**) Differentiation efficiency was quantified by calculating the percentage of MyHC positive nuclei in total nuclei at day 8 ($n = 4$). (**E–H**) RT-qPCR analysis of all clones at day 0 (undifferentiated) and day 8 (differentiated) ($n = 3$) for (E) pluripotency markers, (**F**) myogenic markers, (**G**) DUX4 and its downstream targets and (H) *ACTB* as a reference gene. Relative expression levels were normalized to *RPLP0* as an internal control in each sample and then to F1#1 at day 8 (differentiated). Data information: in (D–H), data are represented as mean ± standard error of the mean.

and C). The results of the reverse-transcription quantitative polymerase chain reaction (RT-qPCR) analysis for pluripotency markers (*OCT3/4*, *NANOG* and *SOX2*) and muscle-lineage markers (*MYOG*, *MYH3* and *CKM*) confirmed the efficient myogenic differentiation of each cell line (Fig. 1E and F; Supplementary Material, Fig. S1D and E). Moreover, RT-qPCR analysis for *DUX4* and its reported downstream targets (*ZSCAN4*, *TRIM43* and *MBD3L2*) revealed considerably higher expression of these molecules in the differentiated state than in the undifferentiated state in the F1 and F2 clones but not in the HC clone (Fig. 1G; Supplementary Material, Fig. S1F). The expression of *ACTB*, which we used as another reference gene, was almost comparable between the undifferentiated and differentiated states (Fig. 1H; Supplementary Material, Fig. S1G). In the case of the F1#1 clone, DNA methylation analysis specific for the allele harboring short D4Z4 repeats revealed that DNA methylation was stably low during the reprogramming from fibroblasts to iPSCs or differentiation from iPSCs to myocytes as compared to the healthy level (> 26%) reported previously by using the same methods (Fig. S2) (34). These data suggested that the myocytes differentiated from the human iPSC clones were suitable for investigating FSHD-related *DUX4* expression.

Downloaded from https://academic.oup.com/hmg/advance-article-abstract/doi/10.1093/hmg/ddy293/5068614 by Kyoto Daigaku Nogaku-bu Toshoshitsu user on 21 September 2018

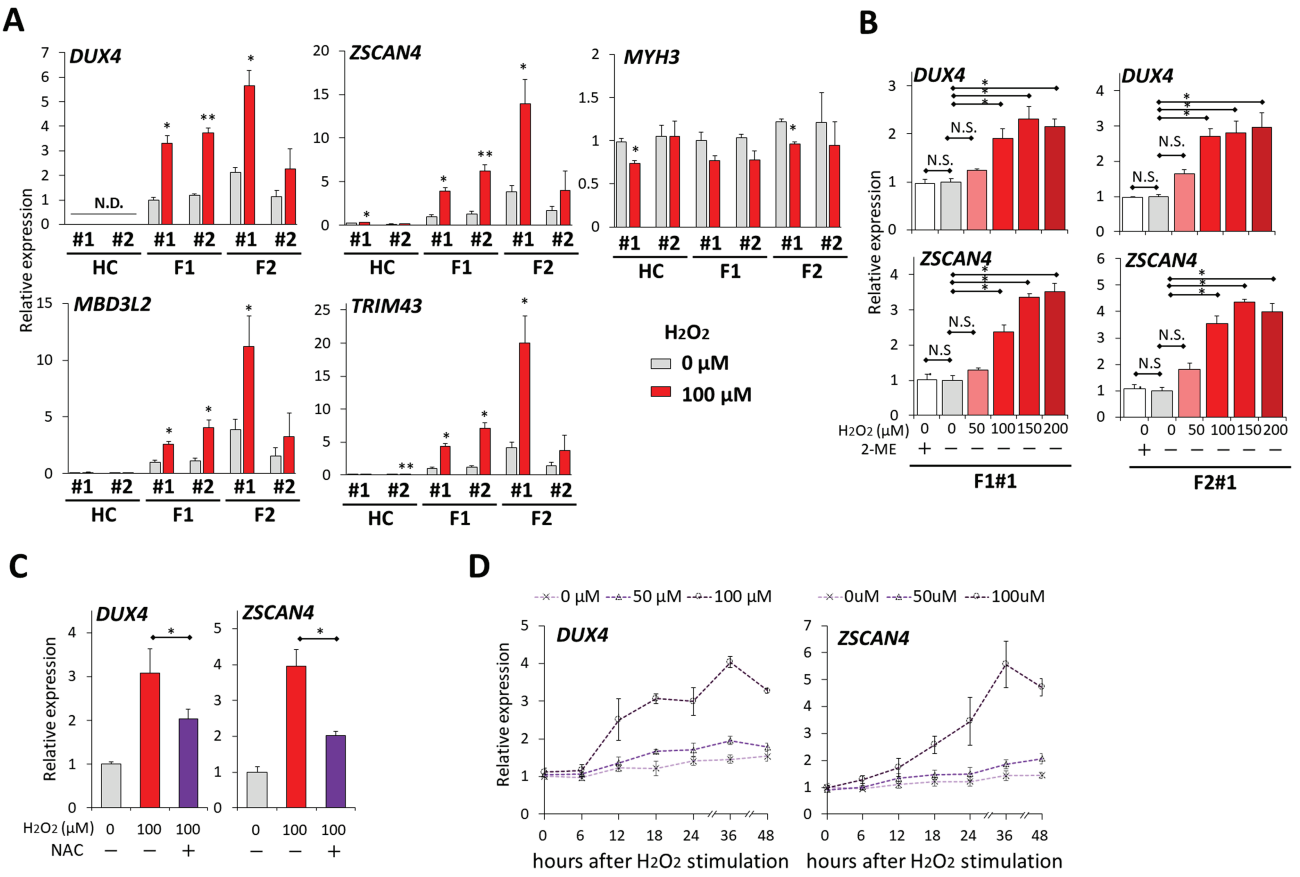

Figure 2. OS increased DUX4 expression in FSHD myocytes. (**A**) RT-qPCR was performed for *DUX4*, its downstream targets (*ZSCAN4*, *TRIM43* and *MBD3L2*) and *MYH3* in HC#1, HC#2, F1#1, F1#2, F2#1 and F2#2 myocytes incubated with or without 100 μM H_2O_2 for 24 h at day 8 after differentiation ($n = 3$ for each condition). Relative expression levels were normalized to *RPLP0* as an internal control in each sample and then to F1#1 without H_2O_2. (**B**) RT-qPCR was performed for *DUX4* and *ZSCAN4* in F1#1 and F2#1 myocytes incubated with 2-mercaptoethanol (2-ME) or with H_2O_2 at various concentrations for 24 h at day 8 after differentiation ($n = 3$ for each condition). Relative expression levels were normalized to *RPLP0* as an internal control in each sample and then to the condition with 0 μM H_2O_2 without 2-ME in each clone. (**C**) NAC was pretreated 1 h before H_2O_2 stimulation to F1#1 myocytes at day 8. 24 h after H_2O_2 addition, RT-qPCR was performed for *DUX4* and *ZSCAN4* ($n = 3$ for each condition). Relative expression levels were normalized to *RPLP0* as an internal control in each sample and then to the condition without H_2O_2 or NAC. (**D**) Time-course analysis of *DUX4* and *ZSCAN4* mRNA expression by RT-qPCR after H_2O_2 stimulation ($n = 3$ per each time point). Relative expression levels were normalized to *RPLP0* as an internal control in each sample and then to the condition with 0 μM H_2O_2. Data information: all data are represented as mean ± SEM. $^*P \leq 0.05$, $^*P \leq 0.01$ [Student's t-test in (A) and (C), one way ANOVA followed by Dunnett's Multiple Comparison Test in (B)].

OS increased DUX4 expression in both FSHD1 and FSHD2 myocytes

To investigate whether OS increases *DUX4* expression, we stimulated myocytes with H_2O_2, which served here as an OS model. RT-qPCR analysis of *DUX4* mRNA expression in myocytes showed that H_2O_2 stimulation for 24 h, which is physiologically mild to allow cell survival (for more than 80%), significantly increased the transcription of *DUX4* and its targets, a phenomenon not observed in the healthy control (Fig. 2A; Supplementary Material, Fig. S3). The H_2O_2 stimulation did not increase the *MYH3* level, indicating that the DUX4 increase was not because of accelerated myogenic differentiation, as DUX4 expression is known to increase after myogenic differentiation (Fig. 2A). F1#1 and F2#1 myocytes showed an almost dose-dependent increase of *DUX4* expression and transcriptional activity (Fig. 2B). Conversely, treatment with NAC, an antioxidant, attenuated the *DUX4* increase induced by H_2O_2, indicating that the OS caused by H_2O_2 stimulation was responsible for the *DUX4* increase (Fig. 2C). Time-course analysis further revealed that the increase of *DUX4* transcription started between 6 and 12 h after H_2O_2 stimulation, suggesting that an early response to OS mediates the increase in transcription (Fig. 2D). The increase of *ZSCAN4* occurred later than the increase of DUX4, suggesting that the DUX4 increase was because of an increase in the amount of transcription per cell, not because of selection for the population with higher DUX4 expression (Fig. 2D). In contrast, F1 fibroblasts did not express *DUX4* regardless of H_2O_2 stimulation (Supplementary Material, Fig. S4). These data demonstrated that OS increased *DUX4* expression in FSHD muscle cells.

DUX4 expression in FSHD2 isogenic control clones showed basal suppression and resistance to OS

To ascertain whether the OS-induced *DUX4* increase was a disease-specific event, we generated isogenic control cell lines by correcting the *SMCHD1* mutation in F2#1 $iPS^{tet\text{-}MyoD}$ cells by using the CRISPR/Cas9 system together with donor template vectors for homology-directed repair (Fig. 3A). Patient F2 carried a heterozygous mutation with a 15 bp deletion and 1 bp substitution in exon 32 of *SMCHD1*, which was modified to generate two isogenic clones (IC#1 and IC#2) in which the mutations were replaced with the wild-type sequence (Fig. 3A and B). These isogenic clones retained the expression of pluripotency markers and exhibited comparable ability to

Downloaded from https://academic.oup.com/hmg/advance-article-abstract/doi/10.1093/hmg/ddy293/5068614 by Kyoto Daigaku Nogaku-bu Toshoshitsu user on 21 September 2018

differentiate into MyHC-positive myocytes (Fig. 3C–E and G–H). SMCHD1 protein expression was increased in isogenic control myocytes compared to parental F2#1 myocytes, indicating haploinsufficiency of SMCHD1 in the parental clone myocytes (Fig. 3F). In IC#1 and IC#2 myocytes, *DUX4* and its downstream targets were expressed at substantially lower levels than in parental clone F2#1 myocytes, indicating that the *SMCHD1* mutation was responsible for the basal *DUX4* transcription in these F2 myocytes (Fig. 3I). Comparable *ACTB* expression confirmed these observations (Fig. 3J). Moreover, the myocytes differentiated from the isogenic control clones showed only a slight increase in *DUX4* expression following H_2O_2 stimulation, and the expression level in the isogenic control clones treated with the highest concentration of H_2O_2 was still lower than that in the parental clone without stimulation (Fig. 3K; Supplementary Material, Fig. S5A). Together, these data indicate that the *DUX4* expression level and its marked OS-induced increase were dependent on the disease-causing *SMCHD1* mutation in FSHD2.

Heterochromatic status at 4q35 was partially increased in F2 isogenic control myocytes

FSHD 4q35 is characterized by chromatin relaxation through DNA hypomethylation and reduced levels of H3K9me3 and HP1γ (4,5). Unexpectedly, DNA methylation in the 4qA allele was not significantly increased after the gene correction (Fig. 4A; Supplementary Material, Fig. S5B). However, chromatin immunoprecipitation (ChIP) followed by RT-qPCR analysis revealed that the accumulation of H3K9me3 and HP1γ had increased in the D4Z4 regions in isogenic control myocytes, whereas H3K4me2, which we used as a transcriptional activation marker, was not significantly altered (Fig. 4B; Supplementary Material, Fig. S5C). Moreover, SMCHD1 accumulation was also increased in isogenic control myocytes, indicating *SMCHD1* haploinsufficiency at the D4Z4 region in the F2 clone (Fig. 4B; Supplementary Material, Fig. S5C). These data indicated that a reduction of heterochromatic histone modification underlays the *DUX4* basal expression and increase by OS in FSHD myocytes.

DDR occurred before DUX4 increase under OS

Because H_2O_2 stimulation exerts a broad range of effects on cells including DNA damage (23,35), we next investigated whether DDR was involved in the OS-induced increase of *DUX4*. At 6 h after H_2O_2 stimulation, when *DUX4* expression was not yet affected by H_2O_2 in FSHD myocytes (Fig. 2D), the expression of γ-H2AX, an indicator of DDR, was increased in each clone similarly (Fig. 5A and B). For F1#1 myocytes, the expression of γ-H2AX showed an H_2O_2 dose-dependent increase (Fig. 5C and D). These data indicate that the DDR by OS occurs prior to DUX4 increase in FSHD myocytes.

Other genotoxic stresses increased DUX4 expression in FSHD myocytes

Moreover, because ultraviolet C (UV-C) exposure induces DDR, we examined its effect and found that a short exposure of myocytes to UV-C (such that most cells survived for 24 h) also increased the expression of *DUX4* and its targets, but not of *MYH3* (Supplementary Material, Fig. S6A–C). The expression of γ-H2AX was similarly increased in each clone before UV-C affected DUX4 transcription (Supplementary Material, Fig. S6D and E). We examined whether DNA damage alone is sufficient to induce the *DUX4* increase using mitomycin C (MMC), a DNA damage inducer. Myocytes treated with MMC also showed an increased expression of *DUX4* and its targets, but not of *MYH3* (Fig. 6A and B). F1#1 myocytes showed an MMC dose-dependent increase of *DUX4* expression and transcriptional activity (Fig. 6C). The expression of γ-H2AX was increased in each clone similarly before MMC affected DUX4 transcription (Fig. 6D and E). These data indicated that genotoxic stresses could increase *DUX4* expression in FSHD myocytes.

OS indirectly increased *DUX4* through ATM-mediated DDR

DDR is primarily controlled by three phosphoinositide 3-kinase-related kinases: ATM, ATM and Rad3-related (ATR) and DNA-dependent protein kinase (DNA-PK) (36,37). To identify the kinase that is responsible for OS-induced *DUX4* increase, F1#1 myocytes were stimulated with H_2O_2 in the presence or absence of specific kinase inhibitors. Whereas the inhibition of ATR or DNA-PK did not markedly affect *DUX4* expression, the inhibition of ATM attenuated the *DUX4* increase induced by H_2O_2 in a concentration-dependent manner (Fig. 7A). Moreover, treatment with the ATM inhibitor caused a decrease in the number of γ-H2AX-positive nuclei under the OS condition in F1 myocytes, which indicated that the DDR triggered by H_2O_2 stimulation was prevented by ATM inhibition (Fig. 7B and C). Although OS can directly activate members of the stress-induced MAP kinase family to regulate gene expression (23,38), the inhibition of MEK, JNK or p38 MAPK did not suppress the OS-induced *DUX4* increase; therefore, this increase appeared not to be a direct outcome of stress responses (Supplementary Material, Fig. S7A). Lastly, the *DUX4* increase in F2#1 myocytes under the OS condition was also attenuated by the ATM inhibitor (Fig. 7D) and inhibition of ATM did not decrease expression of *DUX4* and *ZSCAN4* in FSHD myocytes in the absence of OS (Supplementary Material, Fig. S7B and S7C). Overall, these data indicated that DDR mediates the OS-induced *DUX4* increase through ATM activation in FSHD myocytes.

Discussion

FSHD is caused by genetic disorders but shows variations in disease progression among patients, suggesting the existence of certain external factors that modulate the pathological condition. Using patient iPSCs, this study has demonstrated, to our knowledge for the first time, that the expression of *DUX4*, the gene primarily responsible for FSHD pathology, is increased by external cellular stress. Furthermore, we have shown that the *DUX4* increase induced by OS is mediated by the DDR signaling pathway, which suggests that diverse types of genotoxic stress can increase DUX4 expression and could therefore represent risk factors for FSHD onset or progression.

The involvement of OS in FSHD pathology has been previously reported by several groups. DUX4-expressing muscle cells showed transcriptome enrichment in OS-related gene expression (30–32). Moreover, exogenous DUX4 expression in mouse myoblasts or human immortalized myoblasts resulted in vulnerability to OS (28,39). Endogenous DUX4 expression in immortalized FSHD myoblasts also led to vulnerability to OS and provoked the production of endogenous reactive oxygen species (ROS) followed by DDR to cause partial failure in differentiation (29). However, these findings regarding the association of OS with FSHD provide insights only into the downstream consequences of DUX4 expression. In contrast, our results suggest OS and DNA damage could act as upstream inducers of *DUX4* expression

Downloaded from https://academic.oup.com/hmg/advance-article-abstract/doi/10.1093/hmg/ddy293/5068614 by Kyoto Daigaku Nogaku-bu Toshoshitsu user on 21 September 2018

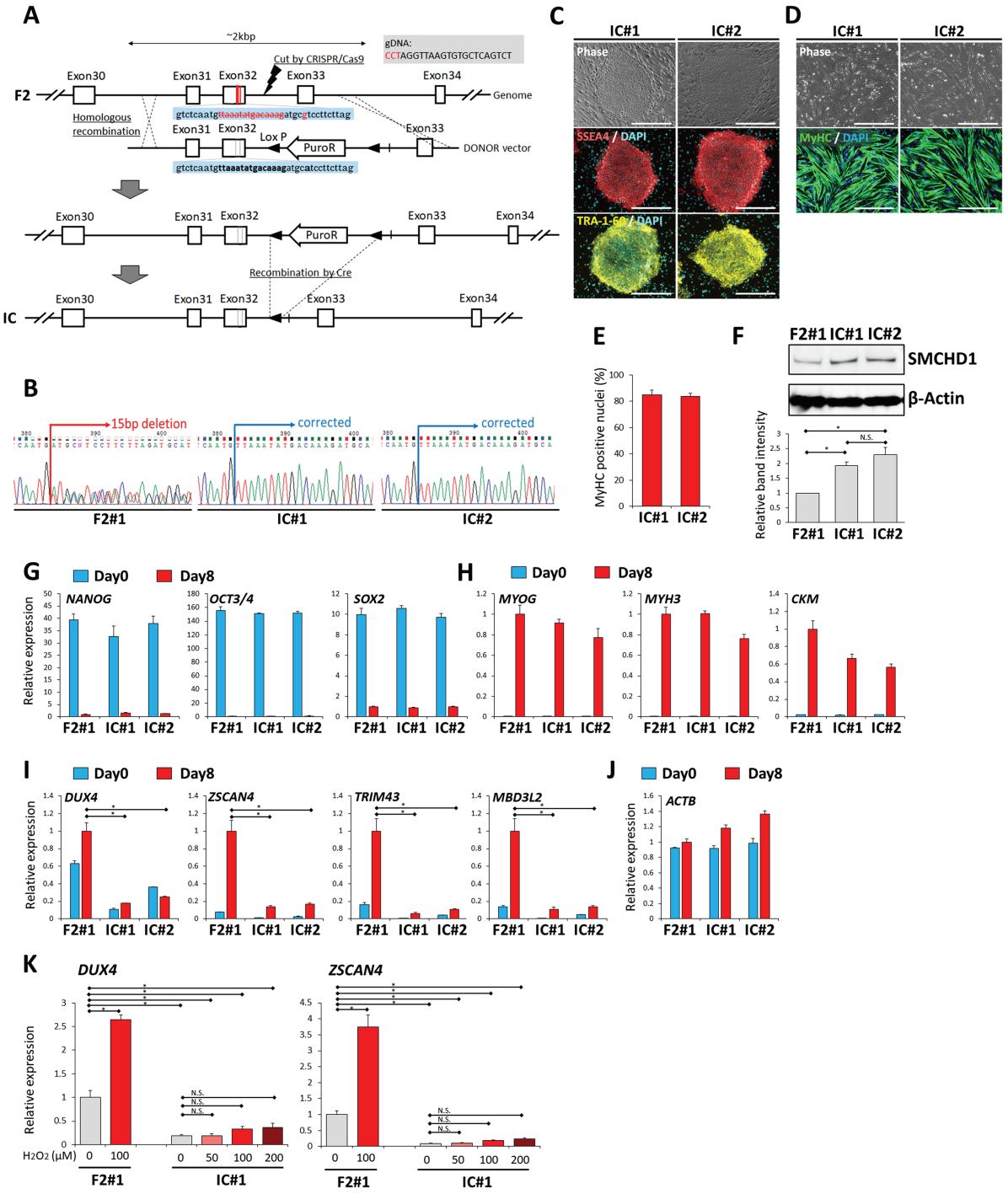

Figure 3. Basal DUX4 expression and increased DUX4 expression by OS were suppressed by gene modification in FSHD2 myocytes. (**A**) Scheme of the gene correction of the SMCHD1 mutation (shown in red letters) in F2 clone. The expected sequence (equal to wild-type sequence) after correction is shown in bold black letters. (**B**) The sequence around the mutation site was checked. F2#1 clone has a heterozygous 15 bp deletion followed by one point mutation (A), resulting in an ambiguous signal pattern, but genetically modified IC#1 and IC#2 clones showed a single pattern consistent with the expected sequence shown in (A), confirming the right correction. (**C**) Representative images of immunofluorescence staining of SSEA4 (red) and TRA-1-60 (yellow) in undifferentiated iPSC$^{tet\text{-}MyoD}$ clones of IC#1 and IC#2. Scale bar: 500 μm. (**D**) Representative images of immunofluorescence staining of MyHC (green) in differentiated myocytes at day 8 of IC#1 and IC#2. Scale bar: 500 μm. (**E**) Differentiation efficiency was quantified by calculating the percentage of MyHC positive nuclei in total nuclei at day 8 ($n = 4$). (**F**) Representative result of western blotting analysis for SMCHD1 (upper panel) and β-Actin (lower panel) in the myocytes of each clone at day 8. The lowest graph shows quantification of relative band intensity. Band intensity of SMCHD1 was normalized to that of β-Actin and subsequently to F2#1 ($n = 3$). (**G–J**). RT-qPCR analysis of all clones on day 0 (undifferentiated) and day 8 (differentiated) ($n = 3$) for (G) pluripotency markers, (**H**) myogenic markers, (I) DUX4 and its downstream targets and (J) *ACTB* as a reference gene. Relative expression levels were normalized to *RPLP0* as an internal control in each sample and subsequently to F2#1 at day8 (differentiated). (**K**) Differentiated myocytes at day 8 after induction from F2#1 and IC#1 clones were incubated with or without H_2O_2 for 24 h, and RT-qPCR was performed for *DUX4* and *ZSCAN4* ($n = 3$ for each condition). Relative expression levels were normalized to RPLP0 as an internal control in each sample and then to F2#1 without H_2O_2. Data information: in (E–K) data are represented as mean ± SEM. *P ≤ 0.05, N. S. not significant [one-way ANOVA followed by Dunnett's Multiple Comparison Test in (I) and by Tukey's test in (F) and (K)].

Downloaded from https://academic.oup.com/hmg/advance-article-abstract/doi/10.1093/hmg/ddy293/5068614 by Kyoto Daigaku Nogaku-bu Toshoshitsu user on 21 September 2018

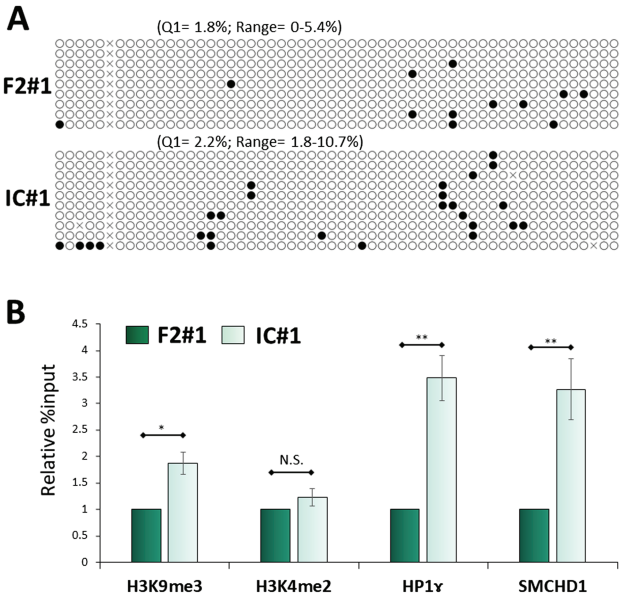

Figure 4. The 4q35 genome in FSHD2 isogenic control myocytes showed a more heterochromatic state at the protein level. (**A**) DNA methylation analysis on the 4q35 region by bisulfite sequencing. White and black circles mark unmethylated and methylated CpG, respectively. The lower quartile (Q1) and range of the percent methylation are shown above each column. (**B**) ChIP RT-qPCR was performed on 4q35 for H3K9me3, H3K4me2 (as a negative control), HP1γ and SMCHD1 ($n = 4$). Relative % input was normalized to F2#1. Data information: all data are represented as mean ± SEM. $^{*}P < 0.05$, $^{**}P < 0.01$ (Student's t test, unpaired).

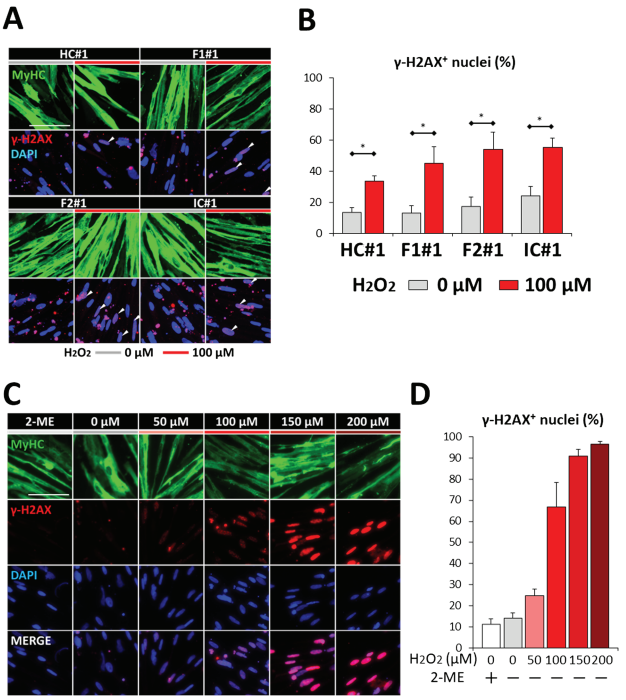

Figure 5. DDR occurred after H_2O_2 stimulation but before DUX4 expression increased. (**A**) Representative images of immunofluorescence staining of MyHC (green) and γ-H2AX (red) in HC#1, F1#1, F2#1 and IC#1 myocytes at day 8 in the presence or absence of H_2O_2. Cells were fixed 6 h after H_2O_2 addition. Scale bar: 100 μm. (**B**) The percentages of γ-H2AX positive nuclei in total nuclei in (A) ($n = 3$). (**C**) Representative images of immunofluorescence staining of MyHC (green) and γ-H2AX (red) in F1#1 myocytes at day 8 incubated with 2-ME or with H_2O_2 at various concentrations for 6 h. Scale bar: 100 μm. (**D**) The percentages of γ-H2AX positive nuclei in total nuclei in (C) ($n = 3$). Data information: in (B) and (D), data are represented as mean ± SEM. $^{*}P \leq 0.05$ [Student's t-test in (B)].

in FSHD. Collectively, these findings indicate that a positive-feedback loop in signaling cascades could be formed among OS, DNA damage and endogenous DUX4 expression. During myogenic differentiation in mouse and human myoblasts, transient DNA strand breakage is followed by the formation of γ-H2AX foci (40,41). This effect might underlie the 'burst' of DUX4 expression in a limited population of FSHD myoblasts during differentiation (20). In the context of differentiated muscle cells, which are recognized to be resistant to diverse stressors (42,43), including H_2O_2 and DNA damage inducers, DNA damage can be accumulated without cell death by suppressing the p53-mediated apoptosis pathway (42,43). This effect might contribute to the increase in *DUX4* expression induced in muscle fibers by OS and other genotoxic stresses. Thus, OS and DNA damage are likely to influence FSHD pathology through the regulation of *DUX4* expression.

ATM performs multiple functions in DDR signaling at DNA lesion sites, including transcriptional regulation and DNA repair. We propose that the diminished heterochromatic state at the 4q35 region, characterized by a reduction of H3K9me3 and HP1γ, increases the region's sensitivity to DNA damage-induced ATM activity, which results in DUX4 increase. A considerable amount of evidence has implicated chromatin compaction in the regulation of ATM activity. HDAC inhibition in human fibroblasts permits an ATM-mediated transcriptional upregulation of MCL1 and Gadd45α, which are ATM targets, through the recruitment of E2F1 transcription factor (44). In the context of DNA repair, heterochromatin serves as a barrier to the expansion of ATM-dependent γ-H2AX (45,46). Moreover, a decrease in chromatin compaction, which can be induced by reducing the level of linker histone H1, enhances resistance to DNA damage through an increased accessibility of DDR factors to the lesion sites (47). Thus, we suggest that non-FSHD 4q35 is transcriptionally silenced and is less sensitive to the DNA damage-induced ATM-mediated transcriptional machinery, whereas FSHD 4q35 permits the ATM-mediated machinery to access the lesion site (Supplementary Material, Fig. S8).

Notably, in our FSHD models, activity of DUX4 was dependent on myogenic differentiation in both types of FSHD and was associated with a disease-related mutation on *SMCHD1* in FSHD2 (Fig. 1G and 3I), which indicates that our models are useful for further FSHD pathological studies. Isogenic controls generated for the FSHD2 clone showed robust suppression of endogenous DUX4 expression, which agrees with previous genetic studies (6). Intriguingly, SMCHD1 was found to recover the heterochromatic state according to the level of a protein marker (although the level was still lower than that in the healthy control; data not shown), but not in terms of the DNA methylation level (Fig. 4). This observation indicates that the DNA methylation status, once determined, remains stable and is resistant to post-developmental modification by epigenetic factors, whereas alterations of heterochromatic protein markers are sufficient to suppress *DUX4* expression at 4q35. This finding supports the modification of histone markers as a therapeutic strategy for FSHD.

Although the expression of DUX4 in FSHD myocytes upregulated downstream transcriptional targets, we did not observe marked phenotypic changes, including apoptosis or impaired differentiation, which apparently disagrees with previous reports (15,21). We propose two possible reasons for this phenotypic absence. The first is that the survival duration of our FSHD myocyte models might be too short to allow for

Downloaded from https://academic.oup.com/hmg/advance-article-abstract/doi/10.1093/hmg/ddy293/5068614 by Kyoto Daigaku Nogaku-bu Toshoshitsu user on 21 September 2018

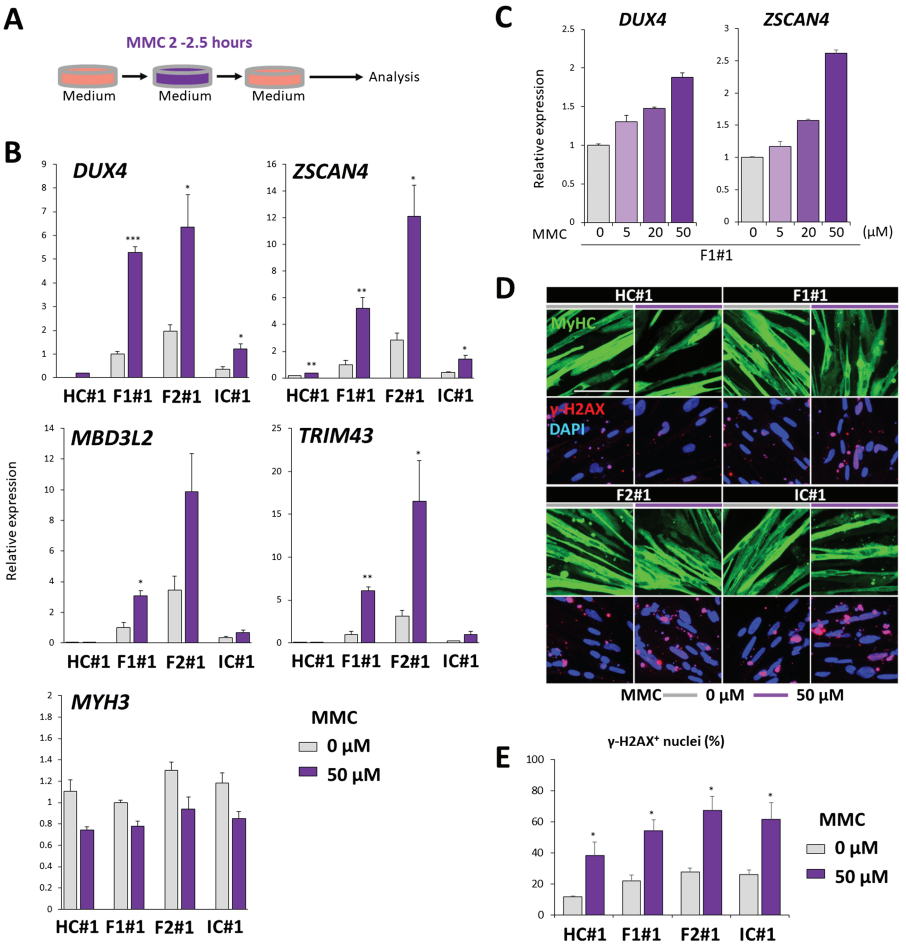

Figure 6. MMC exposure increased DUX4 expression. (**A**) Scheme of the MMC exposure. Differentiated myocytes at day 8 after induction were exposed to MMC for 2–2.5 h, incubated for 9 or 24 h and analyzed. (**B**) RT-qPCR was performed for *DUX4*, its downstream targets (*ZSCAN4*, *TRIM43* and *MBD3L2*), and *MYH3* in HC#1, F1#1, F2#1 and IC#1 myocytes exposed to MMC for 2.5 h and subsequently incubated for 24 h (n = 3 for each condition). Relative expression levels were normalized to *RPLP0* as an internal control in each sample and then to F1#1 without UV-C exposure. (**C**) RT-qPCR was performed for *DUX4* and *ZSCAN4* in F1#1 myocytes exposed to MMC at various concentrations for 2 h and subsequently incubated for 24 h (n = 3 for each condition). Relative expression levels were normalized to *RPLP0* as an internal control in each sample and then to the condition without MMC exposure. (**D**) Representative images of immunofluorescence staining of MyHC (green) and γ-H2AX (red) in HC#1, F1#1, F2#1 and IC#1 myocytes at day 8 exposed to MMC for 2.5 h. Cells were fixed for 9 h after the initiation of MMC exposure. Scale bar: 100 µm. (**E**) The percentages of γ-H2AX positive nuclei in total nuclei in (C) ($n = 3$). Data information: in (B), (C) and (E), data are represented as mean ± SEM. $^{*}P \leq 0.05$, $^{**}P \leq 0.01$, $^{***}P \leq 0.001$ [Student's t-test in (B) and (E)].

notable phenotypic changes under the mild OS conditions used in this study. A higher H_2O_2 concentration therefore may be recommended but at the same time risks cell death independently of DUX4 expression (Supplementary Material, Fig. S3). Instead, a more mature muscle lineage showing longer survival would be preferred. The second is that the myocytes induced in our model system, which was shown to mimic the embryonic myogenic lineage, might maintain resistance to DUX4 activity. Given that DUX4 expression is detected even in the FSHD embryo and that the disease phenotypes manifest long after birth in most FSHD cases (48), embryonic myocytes might be capable of tolerating DUX4 expression. To investigate this possibility, a more mature state of muscle cells could be useful.

In accordance with previous studies, our findings indicate that increased OS is a risk factor for FSHD patients. The elevated OS could potentially be attenuated through supplementation with ROS scavengers or even by including anti-oxidative nutrients in the daily diet. Overall, our study has revealed, by using patient-derived iPSCs, a previously unrecognized mechanism by which *DUX4* expression is regulated in FSHD muscle cells. This finding could provide a basis for drug development and discovery of therapeutic targets for FSHD.

Materials and Methods

Ethical approval

This study was approved by the Ethics Committee of the Graduate School of Medicine, Kyoto University and the Kyoto University Hospital (Approval numbers #R0091 and #G259) and was conducted according to the guidelines of the Declaration of Helsinki. To protect confidentiality, all patient information were kept anonymous, and a written informed consent was obtained from the study participants.

Cell line and cell culture

Human dermal fibroblasts were donated by one Japanese male FSHD1 patient and one healthy donor. Human blood cells were obtained from one Japanese female FSHD2 patient (34). Donor

Downloaded from https://academic.oup.com/hmg/advance-article-abstract/doi/10.1093/hmg/ddy293/5068614 by Kyoto Daigaku Nogaku-bu Toshoshitsu user on 21 September 2018

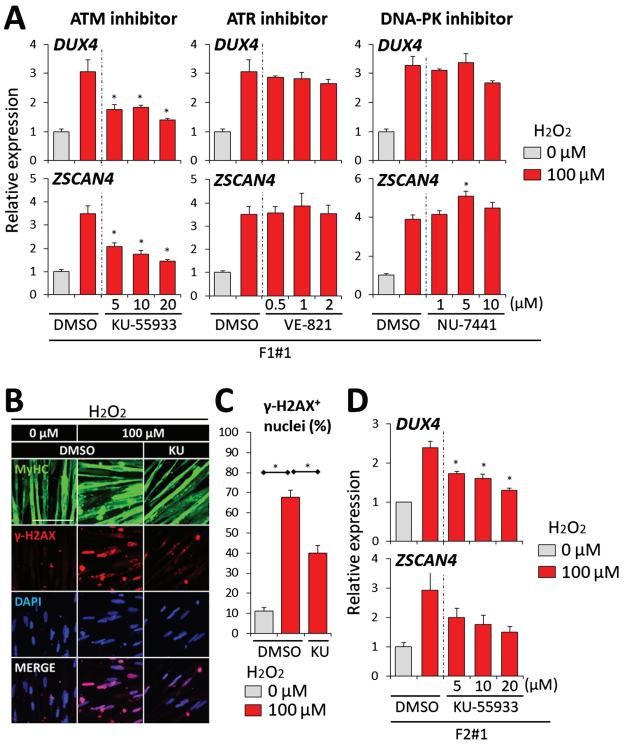

Figure 7. ATM inhibition suppressed DUX4 increase by OS. (**A**) RT-qPCR was performed for *DUX4* and *ZSCAN4* in F1#1 myocytes under H_2O_2 stimulation treated with KU-55933, VE-821 or NU-7441 (inhibitors for ATM, ATR or DNA-PK, respectively) ($n = 3$ for each condition). Relative expression levels were normalized to *RPLP0* as an internal control in each sample and then to the condition with 0 μM H_2O_2. Dimethyl sulfoxide (DMSO) was added to each sample to keep its final concentration comparable among all conditions. (**B**) Representative images of immunofluorescence staining of MyHC (green) and γ-H2AX (red) in F1#1 myocytes in the absence or presence of 100 μM H_2O_2 and 20 μM KU-55933 (KU). DMSO was added to each sample to keep its final concentration comparable among all the conditions. (**C**) The percentages of γ-H2AX positive nuclei in total nuclei in (B) ($n = 3$). (**D**) RT-qPCR was performed for *DUX4* and *ZSCAN4* in F2#1 myocytes under H_2O_2 stimulation and treated with KU-55933 ($n = 3$ for each condition). Relative expression levels were normalized to *RPLP0* as an internal control in each sample and then to the condition with 0 μM H_2O_2. DMSO was added to each sample to keep its final concentration comparable among all conditions. Data information: in (A), (C) and (D), data are represented as mean ± SEM. *$P \leq 0.05$ [one-way ANOVA followed by Dunnett's Multiple Comparison Test in (A), (C) and (D)].

clinical information is listed in Supplementary Table S1. All human iPSCs used in this study were established by overexpressing four transcription factors by using an episomal vector and were maintained on inactivated mouse feeder cells, as previously described (33), in primate embryonic stem (ES) cell medium (ReproCELL, Japan) supplemented with 4 ng/mL recombinant human basic fibroblast growth factor (Oriental Yeast, Japan).

Generation of iPS$^{tet\text{-}MyoD}$ clones

To prepare iPS$^{tet\text{-}MyoD}$ clones (iPSCs that express MyoD in response to doxycycline), the MyoD element was cloned into the PB-TAC-ERN vector by using Gateway cloning to generate PB-MyoD as previously described (33). iPSCs were transfected with plasmids, including PBase and PB-MyoD, by using a NEPA21 electroporator (Nepagene, Japan) and plated on mouse feeder cells for clone selection and culture maintenance as previously described (49).

Myocyte differentiation

iPS$^{tet\text{-}MyoD}$ cells were treated with accutase (Nacalai Tesque, Japan) to separate them into single cells and plated at a density of 3–5 × 10^5 cells/well in 6-well dishes coated with Matrigel (BD Biosciences, USA) in primate ES cell medium supplemented with 100 μg/mL neomycin sulfate (Nacalai Tesque) and 10 μM Y-27632 (Nacalai Tesque). On the following day, the culture medium was replaced with primate ES cell medium containing 1–2.5 μg/mL doxycycline (Dox; LKT Laboratories, USA). Induction was performed in 5% KSR/α-MEM containing Dox and 2-mercaptoethanol (2-ME) supplement for 5–7 days. Dox was removed at least 1 day before harvest for gene expression study.

Correction of SMCHD1 mutation in iPSCs

The mutation in *SMCHD1* was corrected through homologous recombination (HR)-mediated knock-in using the CRISPR/Cas9 system (CRISPR and Cas9 endonuclease system) as described in (50). Briefly, the single-guide RNA (sgRNA) sequence was designed for an intron site near the mutation site by using CRISPRdirect online software (http://crispr.dbcls.jp/) (51) and cloned into pHL-H1-ccdB-mEF1a-RiH (Addgene ID: 60601). For the HR template, bilateral 1 kb regions interposing the sgRNA target site with the mutation in exon 32 replaced by the wild-type sequence were cloned and inserted before and after the puromycin-resistance gene element with two loxP sites in pENTR-Donor-MCS2. The sgRNA vector, the HR vector and pHL-EF1a-SphcCas9-iP-A (Addgene ID: 60599) were cotransfected using a NEPA21 electroporator into F2 iPS$^{tet\text{-}MyoD}$ cells. Subcloning was performed after drug selection for 1 week. Among the obtained clones, those harboring the homozygous HR-derived sequence were selected and transfected with a Cre recombinase construct, and subcloning was again performed to select the clones that had lost the puromycin resistance. Lastly, the sequence was confirmed to contain only one loxP site in each allele. The primers used in these procedures are listed in Supplementary Table S2.

Immunofluorescence analysis

Cultured cells were fixed with 2% formaldehyde in phosphate buffered saline (PBS), washed in PBS, refixed with 100% methanol and blocked with Blocking One solution (Nacalai Tesque) at 4 °C. Fixed samples were incubated overnight at 4 °C with primary antibodies diluted in 10% Blocking One/PBST [PBS containing 0.2% Triton X-100 (Santa Cruz, USA)], washed repeatedly with PBST and incubated for 1 h with secondary antibodies (diluted in 10% Blocking One/PBST) and the nuclear stain DAPI (Sigma; 1:5000). Samples were examined, and images were captured using a BZ9000 system (Keyence, Japan) at 200× and 400× magnification. The antibodies used in this study are listed in Supplementary Table S3. Myocyte differentiation efficiency is shown as the percentage of nuclei within MyHC-positive areas in total nuclei per field.

RNA extraction and real-time RT-qPCR

Total RNA was extracted using a ReliaPrep RNA Miniprep System (Promega) as per the manufacturer's instructions. cDNA was synthesized from the extracted RNA by using ReverTra Ace Master Mix with gDNA Remover (TOYOBO, Japan). Real-time RT-qPCR was performed using SYBR Green probe sets (Applied Biosystems, USA) and a Step One Plus thermal cycler (Applied Biosystems), and a standard curve was prepared for each target.

Downloaded from https://academic.oup.com/hmg/advance-article-abstract/doi/10.1093/hmg/ddy293/5068614 by Kyoto Daigaku Nogaku-bu Toshoshitsu user on 21 September 2018

RPLP0, which encodes a ribosomal protein, was used as the internal control in all assay. The primer sets used in this study are listed in Supplementary Table S4.

Protein extraction and western blotting

Cultured cells were washed with PBS and collected in tubes as pellets. Cell pellets were lysed in radio-immunoprecipitation assay buffer (Nacalai Tesque, Kyoto, Japan) containing 1% (v/v) Protease Inhibitor Cocktail (Nacalai Tesque) and then sonicated with a Bioruptor (BM EQUIPMENT, Japan) for 9 cycles (high intensity, 15/15-s on/off per cycle). Protein concentrations of the lysates were measured using Pierce BCA Protein Assay Kit (Thermo Fisher Scientific, USA) following the manufacturer's instructions. Protein lysate (5 and 1 µg, for SMCHD1 and β-Actin) were mixed with NuPAGE LDS Sample Buffer and NuPAGE Sample Reducing Agent (Thermo Fisher Scientific) and heated at 70°C for 10 min. Samples were then separated on a 3–8% NuPAGE Novex tris-acetate mini gel (Thermo Fisher Scientific) at 150 V for 60 min with the addition of NuPAGE antioxidant (Thermo Fisher Scientific) during electrophoresis. The fractionated proteins were transferred to a polyvinylidene difluoride (PVDF) membrane using an iBlot system (Thermo Fisher Scientific) with the program, P0, 9 min. The membrane was blocked with Blocking One (Nacalai Tesque) and incubated with primary antibody against SMCHD1 (Sigma-Aldrich, USA) at 4°C overnight, otherwise the membrane was blocked overnight for β-Actin. After three washes with PBST (containing 0.1% Tween-20), the membrane was incubated for 1 h at room temperature with peroxidase labeled anti-rabbit IgG antibody (Vector Laboratories, USA) as a secondary antibody for SMCHD1 or with anti-β-Actin−Peroxidase antibody (Sigma-Aldrich, USA). Detection was carried out with SuperSignal West Femto substrate (Thermo Fisher Scientific). Visualization of images was performed by ImageQuant LAS 4000 system (GE Healthcare Life Science, UK). Images were analyzed with ImageJ (https://imagej.nih.gov/ij/) to calculate relative band intensity.

ChIP and ChIP qPCR analysis

ChIP analysis was performed by using an EpiScope ChIP Kit (TAKARA, Japan) according to the manufacturer's instructions with partial modifications. Briefly, 2–5 $\times$ 10^6 cells of each iPSC clone were plated and differentiated in 10 cm dishes to obtain equally confluent myocytes. The cells were cross-linked for 5 min at room temperature with 1% formaldehyde and lysed, and the lysates were sonicated with a Bioruptor for 12 cycles (high intensity, 30/30-s on/off per cycle). Fragmented lysates were incubated with antibodies conjugated to mouse IgG magnetic beads (TAKARA) or Dynabeads Protein G (Thermo Fisher Scientific) overnight. The beads were precipitated and washed in a series of buffers supplied in the kit and with DynaMag (Thermo Fisher Scientific). Immunoprecipitated beads and 10% of the input chromatin was purified by reversing the crosslink and treating with RNase A and Proteinase K according to the manufacturer's instructions. RT-qPCR followed by the $\Delta\Delta$Ct method was used to quantify the D4Z4 elements. Relative % input was calculated by dividing the amount of immunoprecipitated chromatin by that of the input and then normalizing relative to the F2 sample. The following primer pair was used for D4Z4 elements: 5′-CCGCGTCCGTCCGTGAAA-3′ and 5′-TCCGTCGCCGTCCTCGTC-3′ (4).

DNA methylation analysis

Genomic DNA was extracted using a GenElute Mammalian Genomic DNA Miniprep Kit (Sigma-Aldrich, USA) as per the manufacturer's protocol, and 500 ng–1 µg of DNA was treated with bisulfite by using an EpiTect DNA bisulfite kit (QIAGEN, Germany) according to the manufacturer's guidelines. For the F1 clone, the methylation level of the FSHD allele was quantified using the pyrosequencing technique as described in (34). Briefly, PCR was performed using a PyroMark PCR Kit (QIAGEN), and 10 µL of the biotinylated PCR product was affinity purified using Streptavidin Sepharose High Performance (GE Healthcare Life Science) and PyroMark Q24 Advanced CpG Reagents (QIAGEN). For the F2 isogenic controls IC#1 and IC#2, PCR and DNA methylation analysis of the 4qA distal region were performed according to the protocol of the 4qA BSS assay as described in (52) for QUMA online software (http://quma.cdb.riken.jp/index_j.html) (53); the analysis was performed using the default parameters.

Reagents

Hydrogen peroxide mixed with a stabilizer (H_2O_2, Sigma) was added at various concentrations by diluting a 1 mM stock immediately before use on day 8 of myocyte differentiation after the depletion of 2ME for 1 day. N-acetylcysteine (NAC) was dissolved in water, and the pH was adjusted to 7.0. NAC was added to the cells 1 h before H_2O_2 stimulation. KU-55933 (Selleck Chemicals, USA), VE-821 (AdooQ BioScience, USA), NU-7441 (Selleck Chemicals), PD0325901 (Cayman Chemical, USA), SP600125 (Selleck Chemicals) and SB203580 (Sigma) were dissolved in DMSO (Sigma) and added 1 h before H_2O_2 stimulation. MMC was added at various concentration for 2 or 2 and a half h and then washed once and replaced with medium.

UV-C irradiation

For the light source of UV-C, the lamps inside the laminar flow cabinet were used. Myocytes that were differentiated on 6 cm dishes were washed once, and medium was replaced with PBS. Myocytes were then positioned on a fixed position inside the laminar flow cabinet, exposed to UV-C, and washed once. Finally, PBS was replaced with medium.

Supplementary Material

Supplementary Material is available at *HMG* online.

Acknowledgements

We are grateful to the donors who gave their cells for the establishment of iPSCs. We thank Dr Kohei Hamanaka and Dr Hiroaki Mitsuhashi for constructive discussion and Dr Takashi Ikeda and Dr Masaki Yagi for technical instruction. Editage (www.editage.jp) proofread an earlier draft of this paper. We also thank Dr Peter Karagiannis for reading the manuscript. M.S.-H. appreciates all the members of his laboratory for kind support because of his physical handicap. M.S.-H. especially appreciates his parents and Mrs. Nao Sasaki, his wife, for generous and unwavering supports.

Conflict of Interest statement. None declared.

Downloaded from https://academic.oup.com/hmg/advance-article-abstract/doi/10.1093/hmg/ddy293/5068614 by Kyoto Daigaku Nogaku-bu Toshoshitsu user on 21 September 2018

Funding

Acceleration Program for Intractable Diseases Research utilizing Disease-specific iPS cells, which were provided by the Japan Agency for Medical Research and Development, AMED (to H.S. and A.H.); the Japan Society for the Promotion of Science KAKENHI (17 J04509 to M.S.-H. and 15H05581 to A.H.); The Intramural Research Grant [29-4] for Neurological and Psychiatric Disorders of National Center of Neurology and Psychiatry and the Fugaku Trust for Medical Research (to R.M.).

References

1. Tawil, R., van der Maarel, S.M. and Tapscott, S.J. (2014) Facioscapulohumeral dystrophy: the path to consensus on pathophysiology. *Skelet. Muscle*, **4**, 12.
2. Daxinger, L., Tapscott, S.J. and van der Maarel, S.M. (2015) Genetic and epigenetic contributors to FSHD. *Curr. Opin. Genet. Dev.*, **33**, 56–61.
3. Lemmers, R.J.L.F., Van der Vliet, P.J., Klooster, R., Sacconi, S., Dauwerse, J.G., Snider, L., Straasheijm, K.R., Van Ommen, G.J., Padberg, G.W., Miller, D.G. *et al.* (2010) A unifying genetic model for facioscapulohumeral muscular dystrophy. *Science*, **329**, 1650–1653.
4. Zeng, W., De Greef, J.C., Chen, Y.Y., Chien, R., Kong, X., Gregson, H.C., Winokur, S.T., Pyle, A., Robertson, K.D., Schmiesing, J.A. *et al.* (2009) Specific loss of histone H3 lysine 9 trimethylation and HP1γ/cohesin binding at D4Z4 repeats is associated with facioscapulohumeral dystrophy (FSHD). *PLoS Genet.*, **5**, e1000559.
5. Lemmers, R.J.L.F., Goeman, J.J., Van der Vliet, P.J., Van Nieuwenhuizen, M.P., Balog, J., Vos-Versteeg, M., Camano, P., Ramos Arroyo, M.A., Jerico, I., Rogers, M.T. *et al.* (2015) Inter-individual differences in CpG methylation at D4Z4 correlate with clinical variability in FSHD1 and FSHD2. *Hum. Mol. Genet.*, **24**, 659–669.
6. Lemmers, R.J.L.F., Tawil, R., Petek, L.M., Balog, J., Block, G.J., Santen, G.W.E., Amell, A.M., Van Der Vliet, P.J., Almomani, R., Straasheijm, K.R. *et al.* (2012) Digenic inheritance of an SMCHD1 mutation and an FSHD-permissive D4Z4 allele causes facioscapulohumeral muscular dystrophy type 2. *Nat. Genet.*, **44**, 1370–1374.
7. Geng, L.N., Yao, Z., Snider, L., Fong, A.P., Cech, J.N., Young, J.M., Van der Maarel, S.M., Ruzzo, W.L., Gentleman, R.C., Tawil, R. *et al.* (2012) DUX4 activates germline genes, retroelements, and immune mediators: implications for facioscapulohumeral dystrophy. *Dev. Cell*, **22**, 38–51.
8. Shadle, S.C., Zhong, J.W., Campbell, A.E., Conerly, M.L., Jagannathan, S., Wong, C.J., Morello, T.D., van der Maarel, S.M. and Tapscott, S.J. (2017) DUX4-induced dsRNA and MYC mRNA stabilization activate apoptotic pathways in human cell models of facioscapulohumeral dystrophy. *PLoS Genet.*, **13**, 1–25.
9. Whiddon, J.L., Langford, A.T., Wong, C.-J., Zhong, J.W. and Tapscott, S.J. (2017) Conservation and innovation in the DUX4-family gene network. *Nat. Genet.*, **49**, 935–940.
10. De Greef, J.C., Lemmers, R.J.L.F., Camaño, P., Day, J.W., Sacconi, S., Dunand, M., Van Engelen, B.G.M., Kiuru-Enari, S., Padberg, G.W., Rosa, A.L. *et al.* (2010) Clinical features of facioscapulohumeral muscular dystrophy 2. *Neurology*, **75**, 1548–1554.
11. Ricci, G., Zatz, M. and Tupler, R. (2014) Facioscapulohumeral muscular dystrophy: more complex than it appears. *Curr. Mol. Med.*, **14**, 1052–1068.
12. Ricci, E., Galluzzi, G., Deidda, G., Cacurri, S., Colantoni, L., Merico, B., Piazzo, N., Servidei, S., Vigneti, E., Pasceri, V. *et al.* (1999) Progress in the molecular diagnosis of facioscapulohumeral muscular dystrophy and correlation between the number of KpnI repeats at the 4q35 locus and clinical phenotype. *Ann. Neurol.*, **45**, 751–757.
13. Statland, J., Donlin-Smith, C., Tapscott, S., Van Der Maarel, S. and Tawil, A. (2015) Milder phenotype in facioscapulohumeral muscular dystrophy patients with the largest residual D4Z4 fragments. *Neurology*, **84**, 2147–2151.
14. Teveroni, E., Pellegrino, M., Sacconi, S., Calandra, P., Cascino, I., Farioli-Vecchioli, S., Puma, A., Garibaldi, M., Morosetti, R., Tasca, G. *et al.* (2017) Estrogens enhance myoblast differentiation in facioscapulohumeral muscular dystrophy by antagonizing DUX4 activity. *J. Clin. Invest.*, **127**, 1531–1545.
15. Block, G.J., Narayanan, D., Amell, A.M., Petek, L.M., Davidson, K.C., Bird, T.D., Tawil, R., Moon, R.T. and Miller, D.G. (2013) Wnt/β-catenin signaling suppresses DUX4 expression and prevents apoptosis of FSHD muscle cells. *Hum. Mol. Genet.*, **22**, 4661–4672.
16. Huichalaf, C., Micheloni, S., Ferri, G., Caccia, R. and Gabellini, D. (2014) DNA methylation analysis of the macrosatellite repeat associated with FSHD muscular dystrophy at single nucleotide level. *PLoS One*, **9**, 1–24.
17. Sharma, V., Pandey, S.N., Khawaja, H., Brown, K.J., Hathout, Y. and Chen, Y.-W. (2016) PARP1 differentially interacts with promoter region of DUX4 gene in FSHD myoblasts. **7**, 95–121.
18. Campbell, A.E., Oliva, J., Yates, M.P., Zhong, J.W., Shadle, S.C., Snider, L., Singh, N., Tai, S., Hiramuki, Y., Tawil, R. *et al.* (2017) BET bromodomain inhibitors and agonists of the beta-2 adrenergic receptor identified in screens for compounds that inhibit DUX4 expression in FSHD muscle cells. *Skelet. Muscle*, **7**, 16.
19. Snider, L., Geng, L.N., Lemmers, R.J.L.F., Kyba, M., Ware, C.B., Nelson, A.M., Tawil, R., Filippova, G.N., van der Maarel, S.M., Tapscott, S.J. *et al.* (2010) Facioscapulohumeral dystrophy: incomplete suppression of a retrotransposed gene. *PLoS Genet.*, **6**, e1001181.
20. Rickard, A.M., Petek, L.M. and Miller, D.G. (2015) Endogenous DUX4 expression in FSHD myotubes is sufficient to cause cell death and disrupts RNA splicing and cell migration pathways. *Hum. Mol. Genet.*, **24**, 5901–5914.
21. Caron, L., Kher, D., Lee, K.L., McKernan, R., Dumevska, B., Hidalgo, A., Li, J., Yang, H., Main, H., Ferri, G. *et al.* (2016) A human pluripotent stem cell model of facioscapulohumeral muscular dystrophy-affected skeletal muscles. *Stem Cells Transl. Med.*, **5**, 1145–1161.
22. Bosnakovski, D., Chan, S.S.K., Recht, O.O., Hartweck, L.M., Gustafson, C.J., Athman, L.L., Lowe, D.A. and Kyba, M. (2017) Muscle pathology from stochastic low level DUX4 expression in an FSHD mouse model. *Nat. Commun.*, **8**, 550.
23. Mason, S. and Wadley, G.D. (2014) Skeletal muscle reactive oxygen species: a target of good cop/bad cop for exercise and disease. *Redox Rep.*, **19**, 97–106.
24. Kozakowska, M., Pietraszek-Gremplewicz, K., Jozkowicz, A. and Dulak, J. (2015) The role of oxidative stress in skeletal muscle injury and regeneration: focus on antioxidant enzymes. *J. Muscle Res. Cell Motil.*, **36**, 377–393.
25. Turki, A., Hayot, M., Carnac, G., Pillard, F., Passerieux, E., Bommart, S., De Mauverger, E.R., Hugon, G., Pincemail, J., Pietri, S. *et al.* (2012) Functional muscle impairment in facioscapulohumeral muscular dystrophy is correlated with oxidative stress and mitochondrial dysfunction. *Free Radic. Biol. Med.*, **53**, 1068–1079.

Downloaded from https://academic.oup.com/hmg/advance-article-abstract/doi/10.1093/hmg/ddy293/5068614 by Kyoto Daigaku Nogaku-bu Toshoshitsu user on 21 September 2018

26. Passerieux, E., Hayot, M., Jaussent, A., Carnac, G., Gouzi, F., Pillard, F., Picot, M.C., Böcker, K., Hugon, G., Pincemail, J. *et al.* (2015) Effects of vitamin C, vitamin E, zinc gluconate, and selenomethionine supplementation on muscle function and oxidative stress biomarkers in patients with facioscapulohumeral dystrophy: a double-blind randomized controlled clinical trial. *Free Radic. Biol. Med.*, **81**, 158–169.
27. Winokur, S.T., Barrett, K., Martin, J.H., Forrester, J.R., Simon, M., Tawil, R., Chung, S.A., Masny, P.S. and Figlewicz, D.A. (2003) Facioscapulohumeral muscular dystrophy (FSHD) myoblasts demonstrate increased susceptibility to oxidative stress. *Neuromuscul. Disord.*, **13**, 322–333.
28. Bou Saada, Y., Dib, C., Dmitriev, P., Hamade, A., Carnac, G., Laoudj-Chenivesse, D., Lipinski, M. and Vassetzky, Y.S. (2016) Facioscapulohumeral dystrophy myoblasts efficiently repair moderate levels of oxidative DNA damage. *Histochem. Cell Biol.*, **145**, 475–483.
29. Dmitriev, P., Bou Saada, Y., Dib, C., Ansseau, E., Barat, A., Hamade, A., Dessen, P., Robert, T., Lazar, V., Louzada, R.A.N. *et al.* (2016) DUX4-induced constitutive DNA damage and oxidative stress contribute to aberrant differentiation of myoblasts from FSHD patients. *Free Radic. Biol. Med.*, **99**, 244–258.
30. Winokur, S.T., Chen, Y.W., Masny, P.S., Martin, J.H., Ehmsen, J.T., Tapscott, S.J., van der Maarel, S.M., Hayashi, Y. and Flanigan, K.M. (2003) Expression profiling of FSHD muscle supports a defect in specific stages of myogenic differentiation. *Hum. Mol. Genet.*, **12**, 2895–2907.
31. Celegato, B., Capitanio, D., Pescatori, M., Romualdi, C., Pacchioni, B., Cagnin, S., Viganò, A., Colantoni, L., Begum, S., Ricci, E. *et al.* (2006) Parallel protein and transcript profiles of FSHD patient muscles correlate to the D4Z4 arrangement and reveal a common impairment of slow to fast fibre differentiation and a general deregulation of MyoD-dependent genes. *Proteomics*, **6**, 5303–5321.
32. Tsumagari, K., Chang, S.-C., Lacey, M., Baribault, C., Chittur, S.V., Sowden, J., Tawil, R., Crawford, G.E. and Ehrlich, M. (2011) Gene expression during normal and FSHD myogenesis. *BMC Med. Genomics*, **4**, 67.
33. Tanaka, A., Woltjen, K., Miyake, K., Hotta, A., Ikeya, M., Yamamoto, T., Nishino, T., Shoji, E., Sehara-Fujisawa, A., Manabe, Y. *et al.* (2013) Efficient and reproducible myogenic differentiation from human iPS cells: prospects for modeling miyoshi myopathy in vitro. *PLoS One*, **8**, e61540.
34. Hamanaka, K., Goto, K., Arai, M., Nagao, K., Obuse, C., Noguchi, S., Hayashi, Y.K., Mitsuhashi, S. and Nishino, I. (2016) Clinical, muscle pathological, and genetic features of Japanese facioscapulohumeral muscular dystrophy 2 (FSHD2) patients with SMCHD1 mutations. *Neuromuscul. Disord.*, **26**, 472.
35. Bou Saada, Y., Zakharova, V., Chernyak, B., Dib, C., Carnac, G., Dokudovskaya, S. and Vassetzky, Y.S. (2017) Control of DNA integrity in skeletal muscle under physiological and pathological conditions. *Cell. Mol. Life Sci.*, **74**, 3439–3449.
36. Blackford, A.N. and Jackson, S.P. (2017) ATM, ATR, and DNA-PK: the trinity at the heart of the DNA damage response. *Mol. Cell*, **66**, 801–817.
37. Christmann, M. and Kaina, B. (2013) Transcriptional regulation of human DNA repair genes following genotoxic stress: trigger mechanisms, inducible responses and genotoxic adaptation. *Nucleic Acids Res.*, **41**, 8403–8420.
38. Torres, M. and Forman, H.J. (2003) Redox signaling and the MAP kinase pathways. *Biofactors*, **17**, 287–296.
39. Bosnakovski, D., Xu, Z., Gang, E.J., Galindo, C.L., Liu, M., Simsek, T., Garner, H.R., Agha-Mohammadi, S., Tassin, A., Coppée, F. *et al.* (2008) An isogenetic myoblast expression screen identifies DUX4-mediated FSHD-associated molecular pathologies. *EMBO J.*, **27**, 2766–2779.
40. Larsen, B.D., Rampalli, S., Burns, L.E., Brunette, S., Dilworth, F.J. and Megeney, L.A. (2010) Caspase 3/caspase-activated DNase promote cell differentiation by inducing DNA strand breaks. *Proc. Natl. Acad. Sci.*, **107**, 4230–4235.
41. Fischer, U., Ludwig, N., Raslan, A., Meier, C. and Meese, E. (2016) Gene amplification during myogenic differentiation. *Oncotarget*, **7**, 6864–6877.
42. Latella, L., Lukas, J., Simone, C., Lorenzo, P., Puri, P.L. and Bartek, J. (2004) Differentiation-induced radioresistance in muscle cells differentiation-induced radioresistance in muscle cells. *Mol. Cell. Biol.*, **24**, 6350–6361.
43. Fortini, P., Ferretti, C., Pascucci, B., Narciso, L., Pajalunga, D., Puggioni, E.M.R., Castino, R., Isidoro, C., Crescenzi, M. and Dogliotti, E. (2012) DNA damage response by single-strand breaks in terminally differentiated muscle cells and the control of muscle integrity. *Cell Death Differ.*, **19**, 1741–1749.
44. Jang, E.R., Choi, J.D., Park, M.A., Jeong, G., Cho, H. and Lee, J.-S. (2010) ATM modulates transcription in response to histone deacetylase inhibition as part of its DNA damage response. *Exp. Mol. Med.*, **42**, 195–204.
45. Cowell, I.G., Sunter, N.J., Singh, P.B., Austin, C.A., Durkacz, B.W. and Tilby, M.J. (2007) γH2AX foci form preferentially in euchromatin after ionising-radiation. *PLoS One*, **2**, 1–8.
46. Kim, J.A., Kruhlak, M., Dotiwala, F., Nussenzweig, A. and Haber, J.E. (2007) Heterochromatin is refractory to γ-H2AX modification in yeast and mammals. *J. Cell Biol.*, **178**, 209–218.
47. Murga, M., Jaco, I., Fan, Y., Soria, R., Martinez-Pastor, B., Cuadrado, M., Yang, S.M., Blasco, M.A., Skoultchi, A.I. and Fernandez-Capetillo, O. (2007) Global chromatin compaction limits the strength of the DNA damage response. *J. Cell Biol.*, **178**, 1101–1108.
48. Ferreboeuf, M., Mariot, V., Bessières, B., Vasiljevic, A., Attié-Bitach, T., Collardeau, S., Morere, J., Roche, S., Magdinier, F., Robin-Ducellier, J. *et al.* (2014) DUX4 and DUX4 downstream target genes are expressed in fetal FSHD muscles. *Hum. Mol. Genet.*, **23**, 171–181.
49. Shoji, E., Sakurai, H., Nishino, T., Nakahata, T., Heike, T., Awaya, T., Fujii, N., Manabe, Y., Matsuo, M. and Sehara-Fujisawa, A. (2015) Early pathogenesis of Duchenne muscular dystrophy modelled in patient-derived human induced pluripotent stem cells. *Sci. Rep.*, **5**, 12831.
50. Li, H.L., Gee, P., Ishida, K. and Hotta, A. (2016) Efficient genomic correction methods in human iPS cells using CRISPR-Cas9 system. *Methods*, **101**, 27–35.
51. Naito, Y., Hino, K., Bono, H. and Ui-Tei, K. (2015) CRISPRdirect: software for designing CRISPR/Cas guide RNA with reduced off-target sites. *Bioinformatics*, **31**, 1120–1123.
52. Jones, T.I., Yan, C., Sapp, P.C., McKenna-Yasek, D., Kang, P.B., Quinn, C., Salameh, J.S., King, O.D. and Jones, P.L. (2014) Identifying diagnostic DNA methylation profiles for facioscapulohumeral muscular dystrophy in blood and saliva using bisulfite sequencing. *Clin. Epigenetics*, **6**, 23.
53. Kumaki, Y., Oda, M. and Okano, M. (2008) QUMA: quantification tool for methylation analysis. *Nucleic Acids Res.*, **36**, 170–175.

Downloaded from https://academic.oup.com/hmg/advance-article-abstract/doi/10.1093/hmg/ddy293/5068614 by Kyoto Daigaku Nogaku-bu Toshoshitsu user on 21 September 2018